Structural modification in swift heavy ion irradiated muscovite mica*

Sheng-Xia Zhang(张胜霞)[1,†], Jie Liu(刘杰)[1,‡], Jian Zeng(曾健)[1], Pei-Pei Hu(胡培培)[2], and Peng-Fei Zhai(翟鹏飞)[1]

[1] *Institute of Modern Physics, Chinese Academy of Sciences (CAS), Lanzhou* 730000, *China*
[2] *University of Chinese Academy of Sciences, Beijing* 100049, *China*

(Received 12 June 2017; revised manuscript received 3 July 2017; published online 20 August 2017)

Two-layer monoclinic (2M) muscovite mica sheets with a thickness of 12 μm are irradiated with Sn ions at room temperature with electronic energy loss $(\mathrm{d}E/\mathrm{d}x)_\mathrm{e}$ of 14.7 keV/nm. The ion fluence is varied between 1×10^{11} and 1×10^{13} ions/cm^2. Structural transition in irradiated mica is investigated by x-ray diffraction (XRD). The main diffraction peaks shift to the high angles, and the inter-planar distance decreases due to swift heavy ion (SHI) irradiation. Dehydration takes place in mica during SHI irradiation and mica with one-layer monoclinic (1M) structure is thought to be generated in 2M mica after SHI irradiation. In addition, micro stress and damage cross section in irradiated mica are analyzed according to XRD data. High resolution transmission electron microscopy (HRTEM) is used on the irradiated mica to obtain the detailed information about the latent tracks and structural modifications directly. The latent track in mica presents an amorphous zone surrounded by strain contrast shell, which is associated with the residual stress in irradiated mica.

Keywords: muscovite mica, swift heavy ion irradiation, latent track, polymorph transition

PACS: 61.82.–d, 61.80.–x **DOI:** 10.1088/1674-1056/26/10/106102

1. Introduction

There are three common ordered polymorphs of muscovite mica, i.e., $(KAl_3Si_3O_{10}(OH)_2)$: two-layer monoclinic (2M), three-layer monoclinic (3T), and one-layer monoclinic (1M).[1] Mica with 2M structure belongs to space group $C_{2/c}$ with lattice parameters of $a = 0.51906$ nm, $b = 0.9008$ nm, $c = 2.0047$ nm, $\beta = 95.757°$.[2,3] It is a typical two-dimensional layered material with an octahedral layer which mainly includes Al atoms embedded between two tetrahedral layers with a composition of $(Si, Al)_2O_5$. The sandwiched structure is not electrically neutral. A layer of K atom is needed to balance the electrical neutrality. Because of its glide plane along the c axis, mica is easy to cleave along the plane (001), giving a clean and flat surface. Due to this property, mica was usually used as a substrate material.[4] Muscovite mica often occurs over a large range of geological conditions. It is a principal constituent of the fine-grained sediments, many of the metamorphic rocks and some classes of salic igneous rocks. The structure of muscovite mica is limited in certain conditions, such as temperature, pressure, etc. Investigation of the stability of mica structure under an extreme environment has great significance for understanding the mineral formation and the geological conditions, which is applicable for geology and archaeology.

Defects and damage induced by energetic heavy ion irradiation in materials have been an interesting research subject.[5–9] Mica is one of the earliest materials to be used to investigate the irradiation effects of swift heavy ions (SHIs) and highly charged ions (HCIs). Etching tracks on mica induced by charged particles were observed first by Price in the 1960s.[10] It was pointed out that the amorphization in irradiated mica was associated with the formation of amorphous latent tracks. Study of latent tracks induced by energetic ion irradiation in materials has been a subject of interest to investigate the radiation sensitivities of materials.[11] Many investigations have focused on the morphology and size of the latent tracks in mica, produced by SHI irradiation. Tracks in mica irradiated by SHIs (the kinetic energies ranging from 0.5 GeV to 2.76 GeV) were observed in the bulk by transmission electron microscopy (TEM)[12] and at the surface by scanning force microscopy (SFM).[13,14] When injected into a material, SHI would simultaneously transfer its energy to the target primarily by inelastic collisions with the electrons and atoms, which caused excitation and ionization processes.[13,15,16] The size and morphology of the tracks in mica were closely linked to electronic energy loss $(\mathrm{d}E/\mathrm{d}x)_\mathrm{e}$.[13,14] Extensive research was carried out to describe the relationship between latent tracks and $(\mathrm{d}E/\mathrm{d}x)_\mathrm{e}$ by track etching, small-angle x-ray[17] and neutron scattering. The increasing of track diameter with $(\mathrm{d}E/\mathrm{d}x)_\mathrm{e}$ rising has been confirmed in SHI irradiated mica experimentally.

However, research of SHI irradiation effects in mica were primarily concentrated either on the morphology and size of the defects on the sample surface, or on the relationship between track diameter and $(\mathrm{d}E/\mathrm{d}x)_\mathrm{e}$ of the incident ions. Few

*Project supported by the National Natural Science Foundation of China (Grant Nos. 11675233 and 11505243).
†Corresponding author. E-mail: zhangsx@impcas.ac.cn
‡Corresponding author. E-mail: j.liu@impcas.ac.cn
© 2017 Chinese Physical Society and IOP Publishing Ltd

studies were conducted on the polymorph transitions in mica during SHI irradiation. Since the x-ray diffraction (XRD) technique is well suited for the phase identification, the determination of unit cell dimensions and also the analysis of some structural imperfections, the XRD analysis and high resolution transmission electron microscopy (HRTEM) observation are combined in this paper to investigate the polymorph transitions and detailed information about latent tracks in irradiated mica. The XRD is used to analyze the structural transition caused by SHIs. HRTEM is applied to the irradiated mica to acquire the latent track images and to confirm the results obtained from the XRD analysis directly. The study of structural modification in heavy ion irradiated mica has important leading meaning for the geological archaeology.

2. Experiment

Muscovite mica samples with a thickness of 12 μm were irradiated at room temperature with energetic Sn ions accelerated by the Heavy Ion Research Facility in Lanzhou (HIRFL) with $(\mathrm{d}E/\mathrm{d}x)_e$ of 14.7 keV/nm. The direction of irradiation was perpendicular to the mica surface along [001]. Ion fluences ranged from 1×10^{11} ions/cm^2 to 1×10^{13} ions/cm^2. Ion flux was kept lower than 10^8 (ions/cm^2)/s. Aluminum foils with a purity of 99.99% were fixed in front of the samples to adjust the ion energy impacting on the mica surface.

To characterize crystal structural transition due to SHI irradiation, both XRD and TEM observation were carried out. The irradiated samples were cleaved into thin pieces and moved to the micro-grid for TEM observation without any other treatment. The TEM (Tecnai G2 F20, FEI) was conducted on the prepared samples with an acceleration voltage of 200 kV. Track diameters were measured on the HRTEM micrographs. The x-ray diffraction D/Max-2400 with a Cu K_α source of wavelength $\lambda = 0.15418$ nm was used to investigate the modification of crystal structure of mica. Scanning range of 2θ varied from 3° to 80 ° in steps of 10 °/min. The voltage and current applied were 40 kV and 100 mA, respectively.

3. Results

3.1. XRD analyses

XRD patterns of mica before and after irradiation by Sn ions with increasing fluences of 1×10^{11}, 1×10^{12}, 5×10^{12}, 7.5×10^{12}, and 1×10^{13} ions/cm^2 are displayed in Fig. 1. Sharp mica (00L) peaks for $L = 2n$ with integer $n = 1, 2, 3, 4, 5, 6, 7$, and 8 are observed in an angular range from 3° to 80°. It is presented that the pristine mica has a good 2M single crystal with the (001) surface orientation (pdf 260911). With the increase of ion fluence, all peaks display similar behaviors that the full widths half maximum (FWHMs) broaden and the intensities decrease greatly, especially at the fluences of 5×10^{12}, 7.5×10^{12}, and 1×10^{13} ions/cm^2 as shown in Fig. 1. Peak broadening is likely to be due to either grain fragment induced by irradiation or the defects formed in the crystalline fraction.

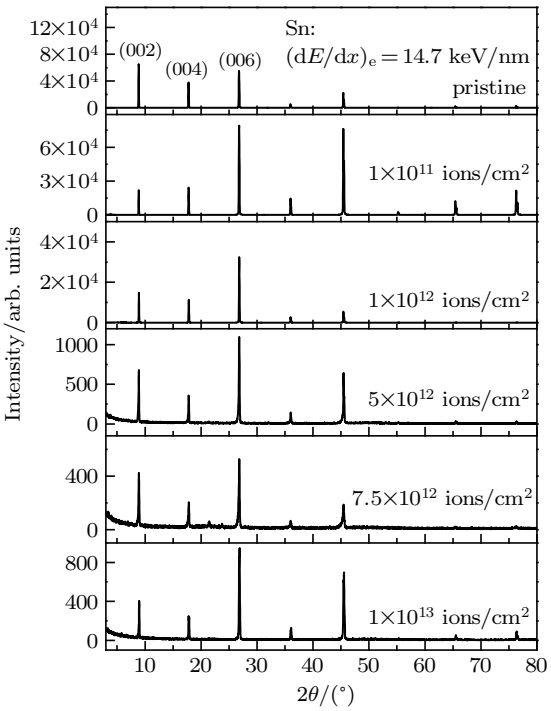


Fig. 1. XRD patterns of mica irradiated by Sn ions at various ion fluences with a $(\mathrm{d}E/\mathrm{d}x)_e$ of 14.7 keV/nm.

The shoulders in the left of the (002) peaks are raised as the samples are irradiated with higher ion fluences, such as 5×10^{12}, 7.5×10^{12}, and 1×10^{13} ions/cm^2 as shown in Fig. 2. Peak fit method is adopted for peak recognition. As fitted in Fig. 2, the broad (002) peak of mica irradiated with higher ion fluences could be decomposed into two peaks. The new peak appearing on the left side of (002) peak was probably the (001) peak of mica with 1M structure (pdf 070025). It is suggested that dehydration proceeds in the pristine mica and partial 2M mica is transformed into 1M mica caused by SHI irradiation.

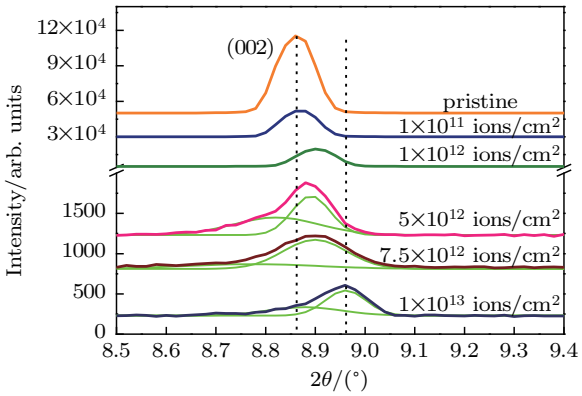


Fig. 2. (color online) Detailed (002) shifting with increasing ion fluence. Dotted lines indicate the shift of (002) with increasing fluence.

The positions of the diffraction peaks are closely related to the atomic arrangements. The position of (002) in 2M mica

shifts to higher 2θ with increasing fluence and other $(00L)$ peaks, as exhibited in Fig. 2. The interplanar distance of (002), $d_{(002)}$, decreases according to the well-known Bragg's law. It is indicated that atoms in the irradiated mica are packed more tightly. The micro stress σ in irradiated mica is estimated from the following equation[18]

$$\sigma = \frac{E}{2\nu}\frac{d_{\mathrm{F}} - d_{\mathrm{c}}}{d_{\mathrm{c}}}, \tag{1}$$

where E and υ are Young's modulus and Poisson ratio of mica, respectively, d_{c} is the original inter-planar distance of (002) measured in the experiment and it is about 1.00 nm, and d_{F} is the distance of (002) with the applied ion fluence F. Elastic modulus of mica adopted in this paper is about 79.3 GPa determined by Zhang *et al.*[19] Mavko *et al.*[20] suggested that Poisson ratio of mica was between 0.23 and 0.28. So, $\upsilon = 0.25$ is adopted in this paper. Micro stress introduced by SHI irradiation is shown in Fig. 3. It is indicated in Fig. 3 that the compressive stress is introduced in the irradiated mica. The value of the micro stress increases gradually with increasing ion fluences.

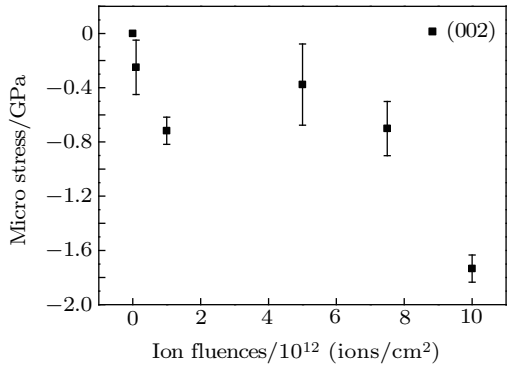


Fig. 3. Micro stresses introduced by Sn ion irradiation with $(\mathrm{d}E/\mathrm{d}x)_{\mathrm{e}}$ of 14.7 keV/nm at different fluences.

Chailley *et al.*[21] measured the latent track radii in ion-irradiated powdered mica with polycrystalline structure by wide-angle XRD. It was explained that there exist three structures in powdered mica after irradiation: an amorphous phase, a crystal structure that remained undisturbed, and a dilated phase, which has the same monoclinical structure of mica but with different values of inter-planar distance d. In this paper, the 'dilated phase' possibly is mica with 1M structure. The kinetics of transformations is obtained through a simplified model in this paper, given the variations of the intensity and of the position of the $(00L)$ XRD reflection peaks with increasing ion fluence. The relationship between the diffraction peak intensity and damage cross-section is given below[22]

$$I_{\mathrm{F}}/I_0 = \mathrm{e}^{-\alpha F}, \tag{2}$$

where I_{F} is the intensity of (002) peak at ion fluence F. As exhibited in Fig. 4(a), the damage cross-section α obtained by fitting I_{F}/I_0, is about 1.3×10^{-12} cm^2 in mica irradiated by Sn ions with $(\mathrm{d}E/\mathrm{d}x)_{\mathrm{e}}$ of 14.7 keV/nm.

The inter-planar distance d decreases after being irradiated by Sn ions in this experiment. Variation of d is fitted with the following formula[22,23]

$$\frac{\Delta d}{d} = \left(\frac{\Delta d}{d}\right)_{\max}(1 - \mathrm{e}^{-\varepsilon F}), \tag{3}$$

where $\Delta d/d = (d_{\mathrm{F}} - d_{\mathrm{c}})/d_{\mathrm{c}}$ and $(\Delta d/d)_{\max} = (d_B - d_{\mathrm{c}})/d_{\mathrm{c}}$.

Here, d_{B} is considered to be the inter-planar distance of the dilated crystal, and d_{F} the average distance of the mica that remained unirradiated and the dilated crystal. For the Sn-ion-irradiated mica, $d_{\mathrm{B}} < d_{\mathrm{c}}$. The ε is the formation cross-section of the 'dilated crystal' in the irradiated mica. As depicted in Fig. 4(b), the plot is graphed against $\Delta d/d$. The formation cross-section ε, derived from the fitting of XRD data in Fig. 4(b), is about $(1.86 \pm 0.60) \times 10^{-13}$ cm^2. As a heavy ion penetrates into the mica sample, damage such as amorphous structure, 'dilated crystal' and other defects would be generated along its path. In this model, damage caused by SHI irradiation is considered to be only amorphous structure and the 'dilated phase' for simplicity. Hence, the radius of the amorphous zone $r \approx 5.9 \pm 1.1$ nm is derived from the relationship: $\alpha - \varepsilon = \pi r^2$. The average diameter of latent tracks extracted from XRD data is about 11.8 ± 1.1 nm, consequently.

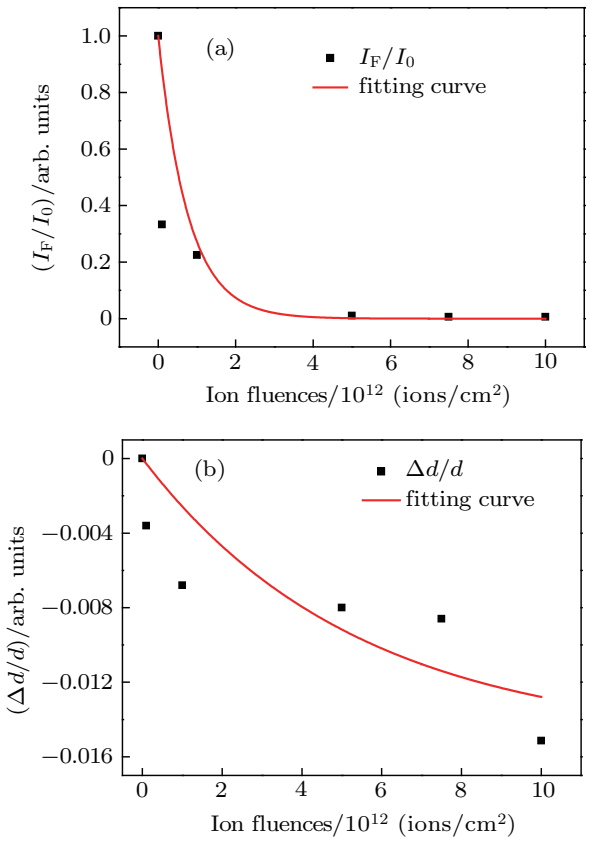


Fig. 4. (color online) Variations of fitting curves of (a) intensity I_{F}/I_0 and (b) inter-planar spacing $\Delta d/d$ of peak (002) with ion fluence.

3.2. Latent tracks

The HRTEM is adopted in this experiment to investigate the defects and structural modification in irradiated mica. Figure 5 shows the HRTEM micrographs of mica irradiated by Sn ions with $(\mathrm{d}E/\mathrm{d}x)_\mathrm{e}$ of 14.7 keV/nm at room temperature, and the fluence is about 1×10^{12} ions/cm^2. The tracks in Fig. 5(a) are uniformly distributed in the cross section image, and the number of the tracks is consistent with the applied ion fluence. The average diameter of latent tracks caused by Sn ion irradiation with $(\mathrm{d}E/\mathrm{d}x)_\mathrm{e}$ of 14.7 keV/nm was about 9.1 ± 1.5 nm, obtained from the HRTEM micrographs. The tracks with amorphous core are surrounded by strain contrast shell as shown in Fig. 5(b). It is suggested that crystal lattice defects form around the ion passage. The structure around the track remains in the regular original crystalline of mica. The strain contrast regions are also oriented in accordance with the crystallographic structure.

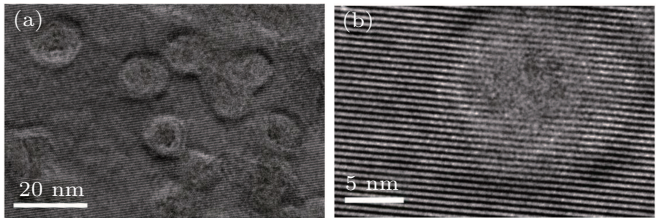


Fig. 5. (a) HRTEM images of muscovite mica subjected to Sn ion irradiation with a $(\mathrm{d}E/\mathrm{d}x)_\mathrm{e}$ of 14.7 keV/nm and an ion fluence of about 1×10^{12} ions/cm^2 (b) enlarged details of tracks.

4. Discussion

Atomic arrangement in muscovite mica is mentioned in Section 1. The XRD is a powerful tool to identify the muscovite polymorphs. It was reported by Yoder and Eugster[24] that 2M structure was more stable at the higher temperatures than the 1M structures during the synthetic process. However, scientists found a dehydration process in phengite under various pressures and temperatures.[25,26] In the thermal spike model, the energy of a heavy ion, lost by the slowing down, is given to the target electrons and then transferred to the lattice through electron–electron and electron–phonon interactions. Electronic energy loss $(\mathrm{d}E/\mathrm{d}x)_\mathrm{e}$ adopted in this experiment is about 14.7 keV/nm, which is above the threshold for bulk damage created in mica. A liquid phase is induced along the ion passage. In the cylinder zone, high pressure and temperature make it convenient to investigate the dehydration process of 2M mica. The conclusion could be verified from the appearance of (001) peak of 1M mica in XRD patterns. The structure of muscovite remains in 2M at lower ion fluences. The 1M structure comes into being at higher fluences as depicted in Fig. 2. In addition, amorphous structures and defects are induced by SHI irradiation, which causes the FWHM of the peaks to increase. Moreover, the K–O bonds are destroyed due to irradiation, which causes the Bragg peaks to shift to higher angles and the inter-distance d to decrease.

The latent tracks observed in the TEM images confirm the XRD results that the amorphous structures and the micro stress are caused by SHI irradiation. Previous experimental investigations have shown the strain field contrast appearing in GeS[12] and InSb[27] around the latent tracks caused by ion irradiation. This phenomenon is closely related to the energy transfer of SHIs reaching the surface of the sample. In the thermal spike model, the amorphous core is produced by the rapid quenching of a cylinder "molten" zone, while the epitaxial structure at the molten/solid interface is associated with residual stress.

5. Conclusions

2M muscovite mica sheets are irradiated by Sn ions with $(\mathrm{d}E/\mathrm{d}x)_\mathrm{e}$ of 14.7 keV/nm at various ion fluences. The TEM observation and XRD analysis are combined to investigate the latent tracks and polymorph transitions in mica. The diffraction peaks shift to higher angles, and the inter-planar distances decrease after irradiation according to the XRD spectra. It is suggested that the amorphous structures and other defects are generated in mica irradiated by SHIs. An increasing trend of the amorphous volume produced in mica irradiated with increasing ion fluences is revealed by XRD analysis. The new peak appearing in the irradiated mica suggests that dehydration takes place during SHI irradiation and pristine mica with 2M structure is transformed into 1M mica. The latent tracks in mica represent an amorphous zone surrounded by strain contrast shell, which is associated with the residual stress in the irradiated mica.

Acknowledgment

We would like to thank all the staff of HIRFL team of the Institute of Modern Physics.

References

[1] Jackson W W and West J 1933 *Z. Kryst.* **83** 160
[2] de Poel W, Pintea S, Drnec J, Carla F, Felici R, Muider P, Elemans J A A W, van Enckevort W J P, Rowan A E and Vlieg E 2014 *Surf. Sci.* **6** 19
[3] Pauling L 1930 *Chemistry* **16** 123
[4] Zheng J, Li Z, Wu A and Zhou H 2003 *Biophys. Chem.* **104** 37
[5] Ding Z N, Yang Y T, Song Y, Zhang L Q, Gou J, Zhang C H and Luo G N 2017 *Acta Phys. Sin.* **66** 112501 (in Chinese)
[6] Zhang C H, Zhang H H, Li B S, Zhou L H, Yang Y T and Fu Y C 2009 *Acta Phys. Sin.* **58** 3302 (in Chinese)
[7] Zeng J, Liu J, Zhang S X, Zhai P F, Yao H J, Duan J L, Guo H, Hou M D and Sun Y M 2015 *Chin. Phys. B* **24** 086103
[8] Zhai P F, Liu J, Zeng J, Yao H J, Duan J L, Hou M D, Sun Y M and Ewing R C 2014 *Chin. Phys. B* **23** 126105
[9] Shen H H, Peng S M, Zhou X S, Sun K, Wang L M and Zu X T 2014 *Chin. Phys. B* **23** 036102
[10] Price P B and Walker R M 1962 *J. Appl. Phys.* **33** 2625

[11] Sun Y M, Liu J, Zhang C H, Wang Z G, Jin Y F, Duan J L and Song Y 2005 *Acta Phys. Sin.* **54** 5269 (in Chinese)
[12] Vetter J, Schloz R, Dobrev D, Nistor L 1998 *Nucl. Instrum. Methods Phys. Res. Sect. B* **141** 747
[13] Ackennann J, Angert N and Neumann R 1996 *Nucl. Instrum. Methods Phys. Res. Sect. B* **107** 181
[14] Ackennann J, Müller A and Neumann R 1998 *Appl. Phys. A* **66** S1151
[15] Toulemonde M, Dufour C and Paumier E 1992 *Phys. Rev. B* **46** 14362
[16] Toulemonde M, Costantini J, Dufour C, Meftah A, Paumier E and Studer F 1996 *Nucl. Instrum. Methods Phys. Res. Sect. B* **116** 37
[17] Toulemonde M, Dufour C and Wang Z 1996 *Nucl. Instrum. Methods Phys. Res. Sect. B* **112** 26
[18] Ferreira N G, Abramof E, Corat E J and Trava-Airoldi V J 2003 *Carbon* **41** 1301
[19] Zhang G, Wei Z and Ferrell R E 2009 *Appl. Clay Sci.* **43** 271
[20] Mavko G, Mukerji T, Dvorkin J 1998 *The Rock Physics Handbook* (Cambridge: Cambridge University Press) p. 208
[21] Chailley V, Bouffard E D S and Balanzat E 1994 *Nucl. Instrum. Methods Phys. Res. Sect. B* **91** 162
[22] Karioris F, Gowda K A and Cartz L 1982 *J. Nucl. Mater.* **108** 748
[23] Weber W 1981 *J. Nucl. Mater.* **98** 209
[24] Yoder H S and Eugster H P 1955 *Geochim. Cosmochim. Acta* **8** 225
[25] Liu Q, Jin Z M and Zhang J F 2009 *Chin. Sci. Bull.* **54** 1455
[26] Cao S H, Zhang L F, Sun Q, Zheng H F and Cui G L 2006 *Acta Petrologica et Mineralogica* **25** 71 (in Chinese)
[27] Szenes G, Horváth Z E, Pécz B, Pászti F and Tóth L 2002 *Phys. Rev. B* **65** 045206